

LETTER

Projection-based Adversarial Attack using Physics-in-the-Loop Optimization for Monocular Depth Estimation

Takeru KUSAKABE[†], Yudai HIROSE[†], *Nonmembers*, Mashiho MUKAIDA[†],
and Satoshi ONO[†], *Members*

SUMMARY Deep neural networks (DNNs) remain vulnerable to adversarial attacks that cause misclassification when specific perturbations are added to input images. This vulnerability also threatens the reliability of DNN-based monocular depth estimation (MDE) models, making robustness enhancement a critical need in practical applications. To validate the vulnerability of DNN-based MDE models, this study proposes a projection-based adversarial attack method that projects perturbation light onto a target object. The proposed method employs physics-in-the-loop (PITL) optimization—evaluating candidate solutions in actual environments to account for device specifications and disturbances—and utilizes a distributed covariance matrix adaptation evolution strategy. Experiments confirmed that the proposed method successfully created adversarial examples that lead to depth misestimations, resulting in parts of objects disappearing from the target scene.

key words: *Adversarial Examples, Monocular Depth Estimation, Physical Attack, Physics-in-the-loop*

1. Introduction

Monocular depth estimation (MDE), which infers three-dimensional data from scenes captured by a single camera [1], has achieved significant performance gains in recent years due to the rapid progress of deep neural networks (DNNs). Currently, this technology finds potential applications in automated material handling in factories and warehouses, as well as in automobile and drone sensing. However, researchers have revealed that DNNs remain vulnerable to adversarial examples (AEs) that induce misclassification through specific perturbations [2], and similar risks affect DNNs used for MDE. When such systems support autonomous robots or self-driving vehicles, misestimations may lead to accidents. Consequently, enhancing the robustness of MDE models is imperative.

In general, adversarial attacks divide into white-box attacks, which use internal information such as model parameters and loss gradients, and black-box attacks, which do not rely on internal data. Given that AI-based services and commercial systems often restrict access to their internal architectures and parameters, black-box attacks are practically valuable for externally assessing system vulnerabilities.

Although early work on adversarial attacks for

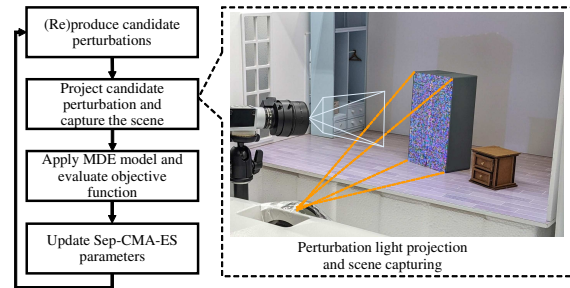


Fig. 1 Overview of the proposed method.

DNNs emphasized digital approaches—such as injecting perturbations or patches into images [3]—current research increasingly investigates physical attacks on real-world objects or scenes [4]. Because these attacks can be performed without compromising the target system, they more accurately reflect practical threat scenarios. Identifying physical adversarial examples not only validates a system’s robustness but also quantifies the maximum disturbances that impair DNN performance.

This paper proposes an adversarial attack method that projects perturbation light onto a target object, thereby triggering misclassifications in MDE systems. Our method harnesses physics-in-the-loop (PITL) optimization [5] to design perturbations by conducting projection and imaging in real-world settings, effectively accounting for environmental complexities. We further integrate Separable Covariance Matrix Adaptation Evolution Strategy (sep-CMA-ES) [8]—recognized as one of the most effective algorithms for high-dimensional black-box optimization—to generate AEs. Experiments confirmed that our method induced significant misestimations that resulted in the disappearance of certain object regions.

2. Related work

Physical adversarial attacks are classified into patch-, camouflage-, and projection-based methods [3]. Patch-based and camouflage-based techniques require direct physical engagement with the target and are thus invasive, whereas projection-based techniques are non-invasive. The non-invasive category is especially alarming as it does not involve direct physical contact with

[†]The author is with the Graduate School of Science and Engineering, Kagoshima University, Korimoto 1-21-40, Kagoshima, 890-0065 Japan.
DOI: 10.1587/transinf.E107.D.1

the object and causes perturbations similar to those produced by natural environmental conditions [6].

Daimo et al. proposed a method to generate AEs for MDE models under black-box conditions [7]. They designed adversarial projection patterns via computer graphics simulation and applied them in a real-world setting. However, performance lagged behind simulation due to difficulty in simulating real-world factors such as reflectance, ambient light, and camera noise.

3. The proposed method

3.1 Key ideas

This paper proposes a projection-based adversarial attack method for MDE models. Compared with patch-based attacks [10], a projection-based attack is limited in the magnitude of perturbation that can be applied; it cannot decrease an object’s surface brightness, and its ability to increase brightness is also constrained, leaving the object’s inherent color influence unavoidable. To mitigate the difficulties associated with projection-based attacks and address the issues in previous work [7], our study introduces key ideas outlined below.

Idea 1: Employing PITL optimization.

The proposed adversarial attack method generates perturbation light patterns by employing PITL optimization, which evaluates candidate solutions under real-world conditions [5]. This method produces adversarial examples that effectively mislead MDE models in real-world environments, eliminating the need to develop simulators that incorporate complex factors like object reflectance and ambient light.

Idea 2: Black-box adversarial attack using Separable Covariance Matrix Adaptation Evolution Strategy (sep-CMA-ES)

Our proposed method employs sep-CMA-ES to achieve global optimization without using the gradient of the objective function, enabling a black-box attack requiring depth maps produced by a victim MDE model. This approach facilitates vulnerability analysis for commercial models, systems, and devices whose internal details are difficult to access. Furthermore, sep-CMA-ES allows us to overcome the limitations of the previous method [7], which relied on combinations of a few local patterns for perturbation generation; the proposed method facilitates the versatile design of perturbations projected onto a target object.

3.2 Formulation

The proposed method generates a light-projection perturbation pattern δ on a target object surface, represented as RGB values; thus, while it can brighten the surface, it cannot darken it. We define the objective function as follows:

Algorithm 1 The proposed attack algorithm

Require: target depth map $\mathbf{d}^{(tgt)}$, victim MDE model h

Ensure: designed perturbation light δ^*

```

1:  $g \leftarrow 1$ 
2: Initialize sep-CMA-ES parameters  $\mathbf{m}^{(1)}$ ,  $\sigma^{(1)}$  and  $\mathbf{C}^{(1)}$ 
3: while  $g \leq g_{max}$  do
4:   for  $k \in \{1, \dots, \lambda\}$  do
5:     Create perturbation, i.e.,  $\delta_k^g \leftarrow \mathcal{N}(\mathbf{m}^{(g)}, \sigma^{(g)2} \mathbf{C}^{(g)})$ 
6:     Project  $\delta_k^g$  to a target object
7:     Capture a scene image  $\mathbf{i}_k^g$ 
8:     Apply MDE model  $h$  to  $\mathbf{i}_k^g$ , i.e.,  $\mathbf{d}_k^{(est,g)} \leftarrow h(\mathbf{i}_k^g)$ 
9:     Calculate  $f(\delta_k^g) = \|\mathbf{d}_k^{(est,g)} - \mathbf{d}^{(tgt)}\|_1$ 
10:  end for
11:   $k_{best} \leftarrow \operatorname{argmin}_k f(\delta_k^g)$ 
12:  if  $f(\delta^*) > f(\delta_{k_{best}}^g)$  then
13:     $\delta^* \leftarrow \delta_{k_{best}}^g$ 
14:  end if
15:  Update  $\mathbf{m}^{(g)}$ ,  $\sigma^{(g)}$ , and  $\mathbf{C}^{(g)}$  according to [8]
16:   $g \leftarrow g + 1$ 
17: end while
18: return  $\delta^*$ 

```

Fig. 2 The proposed algorithm including PITL optimization.

$$\text{minimize } f(\delta) = \sum_{(w,h) \in \mathbf{R}} \left| d_{w,h}^{(est)}(\delta) - d_{w,h}^{(tgt)} \right| \quad (1)$$

where \mathbf{R} denotes a $w \times h$ region on the target object surface, $d_{w,h}^{(tgt)}$ represents the depth at pixel (w, h) in the target depth map, and $d_{w,h}^{(est)}(\delta)$ represents the depth in an estimated depth map when δ is projected.

3.3 Algorithm

Fig. 2 shows the proposed PITL optimization algorithm using sep-CMA-ES. This method searches for the optimal perturbation light δ^* that causes the MDE model h to misestimate the scene depth so that the output resembles a given target depth map $\mathbf{d}^{(tgt)}$.

The proposed method initializes parameters of sep-CMA-ES, including mean vector \mathbf{m} , step size σ , and covariance matrix \mathbf{C} . It subsequently repeats the following steps until reaching the maximum generation g_{max} : sample perturbations $\delta_k^{(g)}$ with $k \in \{1, \dots, \lambda\}$ from a normal distribution \mathcal{N} with parameters $\mathbf{m}^{(g)}$, $\sigma^{(g)}$, and $\mathbf{C}^{(g)}$, i.e., $\delta_k^{(g)} = \mathbf{m}^{(g)} + \sigma^{(g)} \mathbf{y}_k^{(g)}$ where $\mathbf{y}_k^{(g)} \sim \mathcal{N}(\mathbf{0}, \mathbf{C}^{(g)})$; project perturbation $\delta_k^{(g)}$ onto a target object and capture the resulting image \mathbf{i}_k^g ; input \mathbf{i}_k^g into the depth estimator h to obtain an estimated depth map $\mathbf{d}_k^{(est,g)}$; calculate the objective function value; update the best perturbation δ^* and sep-CMA-ES parameters; and generate the next perturbations. Finally, the method outputs the optimal perturbation δ^* .

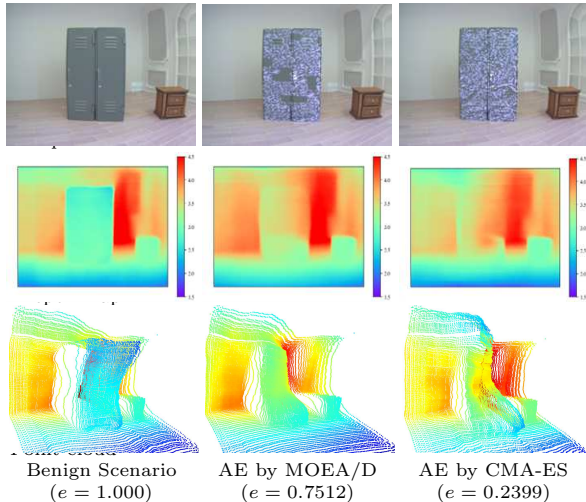


Fig. 3 Exp. 1: Comparison between MOEA/D used in previous work [7] and sep-CMA-ES used in our method.

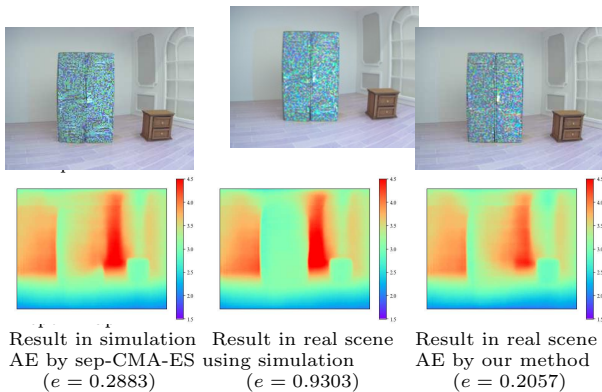


Fig. 4 Exp. 2: Comparison with previous method using simulator [7].

4. Evaluation

To validate our method, we conducted experiments using a real scale model of an indoor scene reproduced at 1/12 of the actual size. In these experiments, we employed a Basler acA1300-30gc camera, a DV3.4X3.8SA-1 lens, and an EPSON EB-E01 projector. We defined the target depth map $\mathbf{d}^{(tgt)}$ as the image captured without the target object and attempted to generate AEs that cause the object to vanish. For sep-CMA-ES, $\mathbf{m}^{(1)}$ was configured so that all RGB values were set to their maximum, and $\sigma^{(1)}$ was set to 1.0. Population size λ was set to $\lambda = 4 + \lfloor 3 \ln n \rfloor$, where n denotes the number of variables ($n = 3|\mathbf{R}|$); thus, λ varies slightly across experiments, ranging from 28 to 32. Other parameters were set to the default values of sep-CMA-ES [8].

Moreover, we quantified object presence by defining a presence rate e as follows:

$$e = \frac{1}{|\mathbf{R}|} \sum_{(w,h) \in \mathbf{R}} \frac{|d_{(w,h)}^{(est)} - d_{(w,h)}^{(back)}|}{|d_{(w,h)}^{(orig)} - d_{(w,h)}^{(back)}|} \quad (2)$$

where $d_{(w,h)}^{(back)}$ denotes the depth value of the background; e equals 1 if the object is fully present and 0 if it completely disappears.

This study validates our method through four experiments: one measuring the effect of using sep-CMA-ES (Exp. 1), another assessing PITL optimization (Exp. 2), a third evaluating performance on low-height objects (Exp. 3), and a fourth evaluating a state-of-the-art MDE model (Exp. 4). Our proposed method performed PITL optimization in real environments across all four experiments. Except for part of Exp. 2, all evaluations were conducted using real scenes.

Exp. 1 compared the sep-CMA-ES optimizer used in our proposed method with MOEA/D algorithm employed in previous work [7], both of which performed PITL optimization. We targeted an MDE model by Laina et al. [9], trained on the NYU Depth v2 indoor scene dataset. Both algorithms were configured with 900 generations and a population size of 28.

Fig. 3 shows the results. Compared with MOEA/D, our method employing sep-CMA-ES produced perturbations that blurred the boundary in the upper locker area, leading to more pronounced object disappearance[†], and it also achieved lower e values. MOEA/D mitigates dimensionality growth through limited local pattern combinations, but this restricts its perturbation diversity, whereas the unconstrained sep-CMA-ES produces more significant misestimations.

Exp. 2 assessed the efficacy of PITL optimization in our proposed method, i.e., integrating solution candidate evaluation using actual devices into the optimization loop, compared to traditional simulation-based evaluation. As in Exp. 1, we employed Laina et al.’s model as the victim model. sep-CMA-ES was configured with $g_{max} = 800$ and $\lambda = 31$.

Fig. 4 illustrates the results: from left to right, it shows the perturbations and estimated depth maps of the AE generated by optimization using simulation-based solution candidate evaluation—assessed in both simulation and real environments—and those of the AE generated by our method. The perturbation that, in simulation, led to misestimations causing the right half of the locker to vanish did not produce such severe misestimations when projected in the actual environment. This discrepancy likely results from differences between simulation and real conditions, yet our PITL approach manages to generate the AE in real settings that is comparable to that from simulation-based optimization.

Exp. 3 investigated the impact of low-height target objects, which a previous study [7] found challenging to misestimate in depth, by employing a kitchen gas stove and a sofa. Consistent with Exp. 1 and 2, we employed Laina et al. model, configuring sep-CMA-ES

[†]Given the inherent difficulty in completely removing a target object in depth estimation, attacks are often judged successful when they cause even a partial object loss [10].

with $\lambda = 30$ and $g_{max} = 800$.

Fig. 5 illustrates the results, which reveal that the attack on the gas stove induced significant misestimations, characterized by a blurred object-background boundary and the vanishing of the left half. In contrast, the attack on the sofa caused nearly complete disappearance of the object, excluding only the armrest that was not perturbed. These results indicate that our method can effectively attack low-height objects.

Exp. 4 aimed to demonstrate our method’s applicability to state-of-the-art MDE models by testing on Depth Anything v2 small model [11]. sep-CMA-ES parameters were set to $\lambda = 32$ and $g_{max} = 1,700$.

Fig. 6 illustrates that, in the absence of projected perturbations, the model correctly captures the spatial relationship in which the target locker is situated in front of a small shelf on its right. However, in the adversarial scene, the estimated depth, except at the locker’s edges, erroneously reaches the wall. These results confirm that our method demonstrates effective attack capability even on modern MDE models.

5. Conclusions

This paper proposed a projection-based adversarial attack method that, under black-box conditions, generates perturbation light projected onto a target object surface to attack MDE models. Our proposed method employed PITL optimization to account for various physical factors—including projector and camera distortions, ambient light, and noise—thus enabling the design of effective perturbation patterns for target scenes. Moreover, using sep-CMA-ES facilitates the versatile design of perturbations projected onto an object surface. Experimental results demonstrated that our method generated adversarial examples resulting in the disappearance of parts of objects.

On the other hand, a drawback of the proposed method is that its perturbations are substantial and perceptible. In the future, we plan to extend our method to reduce the magnitude of perturbations

References

- [1] A. Bhoi, “Monocular depth estimation: A survey,” *arXiv:1901.09402*, 2019.
- [2] I. J. Goodfellow, J. Shlens, and C. Szegedy, “Explaining and harnessing adversarial examples,” *arXiv:1412.6572*, 2014.
- [3] D. Wang, *et al.*, “A survey on physical adversarial attack in computer vision,” *arXiv:2209.14262*, 2022.
- [4] A. Guesmi *et al.*, “Physical adversarial attacks for camera-based smart systems: Current trends, categorization, applications, research challenges, and future outlook,” *IEEE Access*, vol. 11, pp. 109617–109668, 2023.
- [5] T. Minamata *et al.*, “A coded aperture as a key for information hiding designed by physics-in-the-loop optimization,” *IEICE Trans. Inf. Sys.*, vol. 107, no. 1, pp. 29–38, 2024.
- [6] T. Sato, *et al.*, “Invisible reflections: Leveraging infrared laser reflections to target traffic sign perception,”

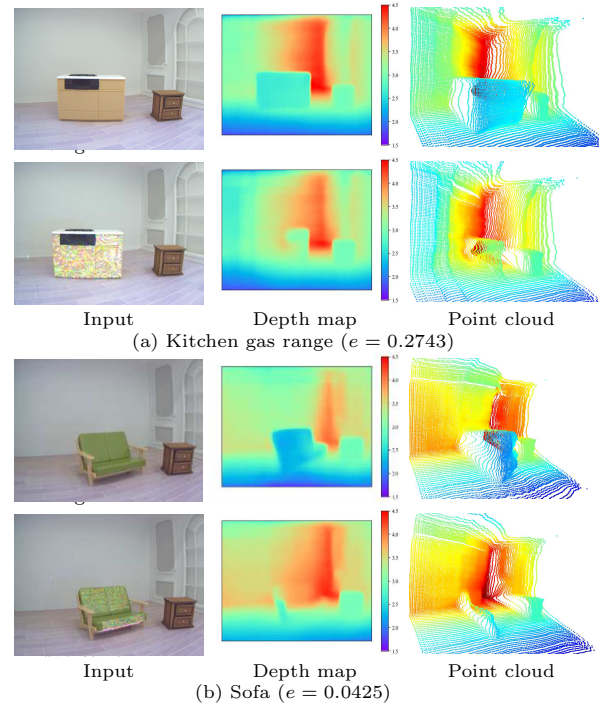


Fig. 5 Exp. 3: results against other objects.

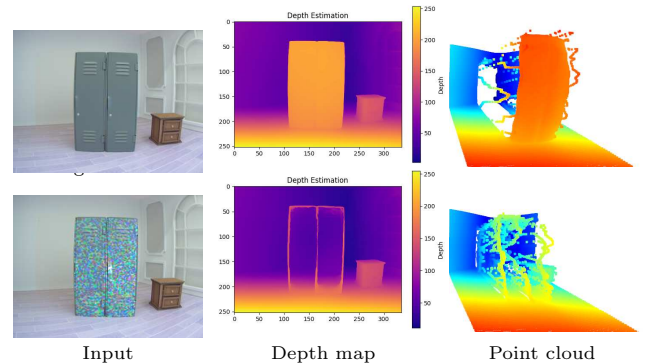


Fig. 6 Exp. 4: attack to state-of-the-art MDE model Depth Anything v2 ($e = 0.312$).

arXiv:2401.03582, 2024.

- [7] R. Daimo and S. Ono, “Projection-based physical adversarial attack for monocular depth estimation,” *IEICE Trans. Inf. Sys.*, vol. E106.D, no. 1, pp. 31–35, 2023.
- [8] R. Ros and N. Hansen, “A simple modification in CMA-ES achieving linear time and space complexity,” in *Int’l Conf. Parallel Problem Solving from Nature*, pp. 296–305, 2008.
- [9] I. Laina, *et al.*, “Deeper depth prediction with fully convolutional residual networks,” in *Int’l Conf. 3D Vision*, pp. 239–248, 2016.
- [10] Z. Cheng, *et al.*, “Physical attack on monocular depth estimation with optimal adversarial patches,” in *Europ. Conf. Computer Vision*, pp. 514–532, 2022.
- [11] L. Yang, *et al.*, “Depth Anything v2,” *Advances in Neural Inf. Proc. Sys.*, vol. 37, pp. 21875–21911, 2025.